



REVIEW

Single-neuron axonal reconstruction: The search for a wiring diagram of the brain

Michael N. Economo  | Johan Winnubst | Erhan Bas | Tiago A. Ferreira  | Jayaram Chandrashekar

Janelia Research Campus, Howard Hughes Medical Institute, Ashburn, Virginia

Correspondence

Michael N. Economo, Janelia Research Campus, Howard Hughes Medical Institute, Ashburn, VA.

Email: economom@janelia.hhmi.org and

Jayaram Chandrashekar, Janelia Research Campus, Howard Hughes Medical Institute, Ashburn, VA.

Email: chandrashekarj@janelia.hhmi.org

Present address

Michael N. Economo, Boston University, Boston, MA

Abstract

Reconstruction of the axonal projection patterns of single neurons has been an important tool for understanding both the diversity of cell types in the brain and the logic of information flow between brain regions. Innovative approaches now enable the complete reconstruction of axonal projection patterns of individual neurons with vastly increased throughput. Here, we review how advances in genetic, imaging, and computational techniques have been exploited for axonal reconstruction. We also discuss how new innovations could enable the integration of genetic and physiological information with axonal morphology for producing a census of cell types in the mammalian brain at scale.

KEYWORDS

axonal reconstruction, long-range circuits, whole-brain imaging

1 | INTRODUCTION

Animal behavior is the product of the coordinated action of diverse brain regions. Brain areas communicate through long-range circuits formed by the axons of projection neurons. The unique axonal projection pattern of an individual neuron determines the subset of brain regions and other cells to which it connects and transmits information. Neuronal morphology—a cell's axonal projection pattern and the shape of its dendritic tree—also represents one of the principal descriptors used to define neuronal cell types. Nevertheless, axonal reconstruction remains a technically challenging endeavor. As a result, complete axonal reconstructions have been produced for only a few types of projection neurons in the mammalian brain.

Recent advances in imaging technologies have permitted the acquisition of high resolution, high signal-to-noise image volumes of the complete rodent brain (Economo et al., 2016; Li et al., 2010; Mayerich, Abbott, & McCormick, 2008; Oh et al., 2014; Ragan et al., 2012). Novel genetic and viral tools enable neurons to be brightly and sparsely marked with fluorescent labels. Computational approaches have accelerated the identification and segmentation of axonal segments within large image volumes. These and other technologies now enable efficient reconstruction of the axonal projections of single neurons. Here, we describe how each of these advances have been exploited for this

purpose and discuss the challenges that must be overcome to understand long-range connectivity in the brain at the single-neuron level.

2 | THE CHALLENGE OF AXONAL RECONSTRUCTION

Mammalian projection neurons possess axonal arbors with complex branching patterns. Axonal projections frequently span large portions of the brain (Economo et al., 2016, 2018; Kita & Kita, 2012; Kuramoto et al., 2009; Li et al., 2018; Ohno et al., 2012; Wittner, Henze, Záborszky, & Buzsáki, 2007; Wu, Williams, & Nathans, 2014) (Figure 1) and include segments that may be less than 100 nm in diameter (Shepherd & Harris, 1998). The complexity and scale of axonal projections has presented a significant hurdle in determining their structure and projection targets.

All existing reconstructions of mammalian neurons have been produced using variations of the same three-step procedure. First, one or more neurons are labeled within the brain. Next, fixed tissue containing the labeled neurons is imaged with light microscopy. Finally, axonal arbors are traced digitally or with pen and paper. Classical implementations of this *labeling-imaging-tracing* paradigm are laborious and rarely produced axonal reconstructions approaching completeness. Here, we discuss several key technological advances

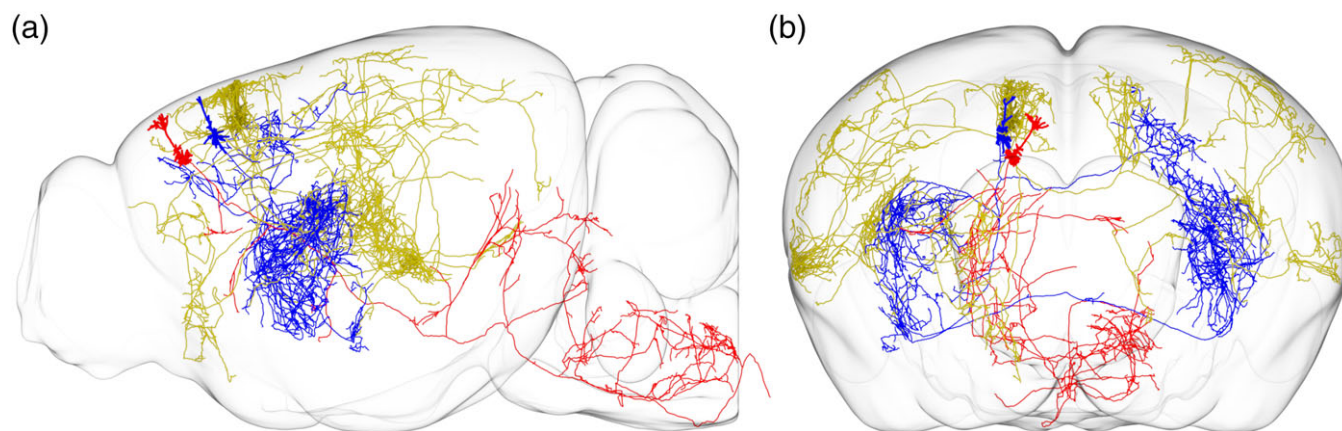


FIGURE 1 Axonal arbor of cortical projection neurons. (a) Three projection neurons in layer 5 of motor cortex collapsed in the sagittal plane. Intratelencephalic neurons projecting to other cortical areas and the striatum display a large degree of projection heterogeneity (yellow, blue). Pyramidal tract neurons connect motor cortex with the midbrain and hindbrain (red). (b) The same three neurons projected in the coronal plane. Reconstructions retrieved from <http://ml-neuronbrowser.janelia.org/>. Total axonal lengths of illustrated neurons are 44.7 cm (yellow; ID: AA0100), 30.1 cm (blue; ID: AA0267), and 13.4 cm (red; ID: AA0180) [Color figure can be viewed at wileyonlinelibrary.com]

for labeling and imaging neurons that have vastly improved the efficiency and completeness of axonal reconstructions.

2.1 | Sparse axonal labeling

Reconstructing axonal projections requires the processes of one neuron to be distinguished from those of surrounding cells. However, the cell membranes of adjacent neurons can be separated by as little as ~20 nm. Adjacent cells can be effectively resolved using electron microscopy, but this approach has only been applied to tissue volumes less than 1 mm³ (Bock et al., 2011; Helmstaedter et al., 2013; Kasthuri et al., 2015)—orders of magnitude smaller than the mouse brain (~400 mm³) (Kovačević et al., 2005). Sparse labeling of neurons relaxes the requirements on the resolution of the imaging system by minimizing “axonal crossovers,” where axons of different cells come into close contact (i.e., separated by less than the resolution of the imaging system; Figure 2). Reducing axonal crossovers with sparse neuronal labeling minimizes the likelihood of topological errors (Chothani, Mehta, & Stepanyants, 2011) and permits reconstruction of neurons with light microscopy.

Sparse labeling first enabled the visualization of the axons of single neurons after the introduction of Camillo Golgi's black reaction, which randomly labeled small numbers of neurons with an opaque precipitate of silver chromate (Golgi, 1873). This advance directly led to the formulation of the neuron doctrine (Ramón y Cajal, 1888), and

the law of dynamic polarization (Ramón y Cajal, 1891), important milestones in our understanding of brain structure and function. In the second half of the 20th century, chromogenic and fluorescent stains like horseradish peroxidase (Cullheim & Kellerth, 1976; Kitai, Kocsis, Preston, & Sugimori, 1976; Snow, Rose, & Brown, 1976), biocytin (Horikawa & Armstrong, 1988), and lucifer yellow (Stewart, 1978; Stuart, Dodt, & Sakmann, 1993) introduced through a glass recording pipette were instrumental for recovering the morphology of neurons labeled during electrophysiological recordings—thereby linking morphological and functional information about single neurons (Cullheim & Kellerth, 1976; Horikawa & Armstrong, 1988; Kitai et al., 1976; Snow et al., 1976). Importantly, axonal labeling using these techniques is typically limited to a single neuron per brain and results in incomplete labeling due to the limited quantity of label that can be introduced into each cell through a pipette.

Genetic and viral tools (Luo, Callaway, & Svoboda, 2008, 2018) have addressed two of the limitations of classic sparse labeling approaches. First, the continuous production of fluorescent proteins within cells encoded by viral DNA or transgenes results in complete labeling of axonal and dendritic processes (Figure 3). Second, the sparsity and identity of labeled neurons may be precisely controlled on the basis of endogenous gene expression patterns (Wu et al., 2014), by delivering viral vectors in a spatially precise manner (Economo et al., 2016; Kuramoto et al., 2009; Li et al., 2018; Ohno et al., 2012), or by local delivery of plasmid DNA directly through a recording

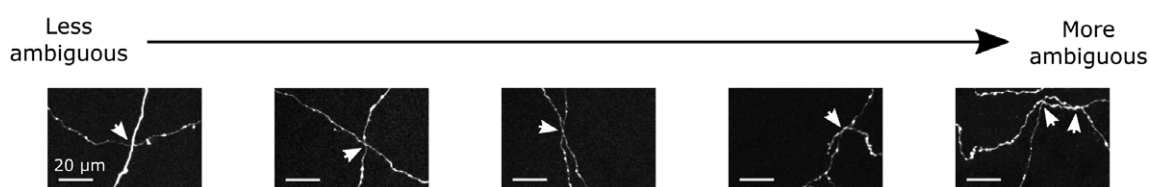


FIGURE 2 Axonal crossovers introduce topological uncertainty. Ambiguity in axonal reconstructions is introduced by axonal crossovers—close appositions of axonal segments from different neurons. Examples of axonal crossovers are subjectively ordered from left to right by the level of uncertainty to which individual fibers can be traced. Examples are two-dimensional projections of three dimensional data and are provided for illustrative purposes only. Adapted from Economo et al. (2016)

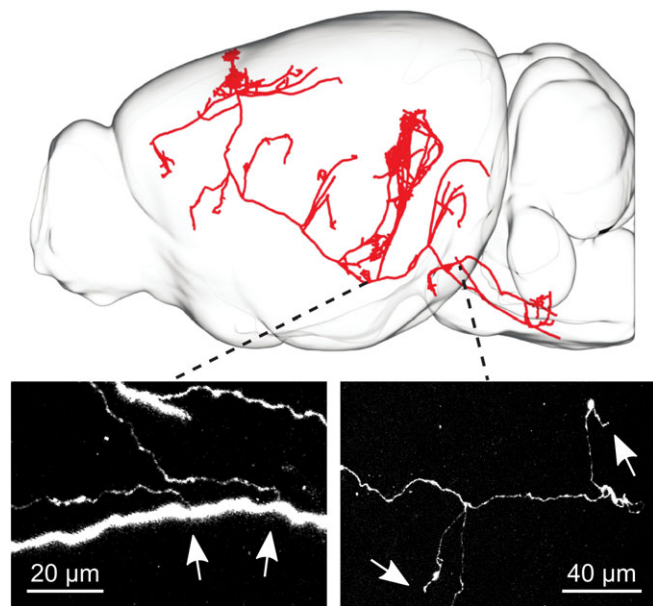


FIGURE 3 Virally expressed fluorescent proteins completely fill axonal arbors. Reconstruction of a pyramidal tract neuron in motor cortex labeled virally with a fluorescent protein. *Bottom, left:* Collateral branches often possess small calibers compared to their parent segments (arrows). *Bottom right:* Fine branches are clearly detectable at the most distal end of the axonal arbor and end in clear terminations (arrows) [Color figure can be viewed at wileyonlinelibrary.com]

pipette (Han et al., 2018; Rancz et al., 2011). These advances have been crucial for permitting high-throughput axonal reconstruction.

2.2 | Axonal imaging

Sparsely labeled axons have classically been visualized and traced across series of thin (~50 µm) tissue sections due to constraints imposed by light scattering in thicker tissue. Serial sections are prone to deformation and damage, and reconstructing neurons across multiple sections is laborious and error-prone.

Automated, high resolution fluorescence imaging of continuous three-dimensional image volumes that span the whole brain has greatly improved the efficiency of axonal reconstruction (Economo et al., 2016). Three imaging approaches have been applied to whole brain fluorescence imaging with sufficient signal-to-noise and resolution to resolve and trace the axons of single neurons. First, knife-edge scanning microscopy (KESM; Mayerich et al., 2008) and fluorescence micro-optical sectioning tomography (fMOST; Gong et al., 2013; Li et al., 2010) both employ diamond knives to simultaneously section and image ~1 mm wide strips of resin-embedded tissue at a thickness of ~1 µm. Images are acquired with widefield microscopy as the sectioned tissue moves across the knife blade. The axial resolution of this method is therefore determined by the sectioning thickness and not the optical system. Variants of this method maintain a reliance on micron-scale sectioning while employing other imaging strategies (Xiong et al., 2014). Second, in serial two photon tomography (STPT), an image, or image volume several hundred microns in depth, near the exposed surface of a formaldehyde-fixed tissue sample is acquired using two-photon excitation microscopy. Tissue (50–400 µm) is then

subsequently removed using an integrated vibratome (Economo et al., 2016; Han et al., 2018; Ragan et al., 2012). In KESM/fMOST and STPT, sectioning and imaging are repeated until images spanning a complete brain are acquired. Third, another approach uses selective plane illumination microscopy (SPIM; Keller & Dodt, 2012; Mertz, 2011; Voie, Burns, & Spelman, 1993) to image optically cleared tissue samples without the need for sectioning (Chung & Deisseroth, 2013; Dodt et al., 2007; Renier et al., 2014; Susaki et al., 2014).

Each of these methods possess distinct advantages and disadvantages for axonal reconstruction. KESM/fMOST do not require high cost laser sources for excitation but rely upon diamond knives that may be difficult to source and maintain. Resin embedding is complex compared to standard formaldehyde fixation and incompatible with many fluorophores. Because overlapping images are not acquired at the edge of each field of view, these methods are prone to loss of data at the edge of each cut. The destructive nature of this approach precludes the repetition of imaging in these locations. STPT requires expensive pulsed femtosecond laser sources and complex, computationally intensive volumetric image stitching to correct for plastic deformation that accompanies each physical section. Acquisition of a complete mouse brain volume requires 5–10 days of continuous imaging time with both KESM/fMOST and STPT, while the equivalent volume may, in principle, be imaged using SPIM in several hours. However, axial resolution is lower using this approach (1–2 µm for KESM/fMOST and STPT vs. 5–20 µm with large-volume SPIM imaging) (Dodt et al., 2007; Keller et al., 2010). Lastly, SPIM may only be performed on optically transparent tissue cleared using chemical methods that can be difficult to effectively apply to adult whole-brain samples.

2.3 | Axonal reconstruction

In serial-section reconstruction, axonal segments are traced with pencil-and-paper and then connected manually or automatically (Ropiredy, Scorcioni, Lasher, Buzsáki, & Ascoli, 2011; Scorcioni & Ascoli, 2005) across sections to assemble the complete axonal arbor. In addition to being error-prone, this process requires weeks or months for the reconstruction of each axonal arbor (Ropiredy et al., 2011; Wittner et al., 2007).

Reconstructing axonal projections within complete image volumes spanning the brain is potentially far more efficient but critically reliant upon a host of computational methods. Image data spanning the brain must be registered (if acquired with STPT), and then resampled into a single axis-aligned image volume in which overlapping regions from different acquisitions are merged (Economo et al., 2015). This image volume is displayed either in two dimensions as an image stack or rendered as a three dimensional volume. Interactive annotation tools allow human annotators to digitally trace the 3D structure of axons within the rendered image volume. Increasingly, machine learning and computer vision techniques are applied before tracing to automate parts of the reconstruction process (Quan et al., 2016; Winnubst et al., 2019). Each of these steps is complicated by the scale of whole-brain image volumes; mouse brain datasets easily reach many teravoxels at the resolution necessary for tracing axons. The magnitude of these data have required the development of computational pipelines in which data transfer and compute times are not prohibitively large.

Algorithmic approaches for extracting axonal and dendritic morphologies from light microscopic datasets have been developed for over half a century (Glaser & Loos, 1965; Meijering, 2010) and continue to be the subject of intense research (Peng et al., 2015). In 2010, the Digital reconstruction of Axonal and Dendritic Morphology (DIADEM) competition solicited algorithmic approaches for tracing axons and dendrites in small datasets acquired with fluorescence microscopy (Ascoli, 2008). At that time, all evaluated algorithms required substantial post hoc error correction and were unable to achieve the goal of a 20× reduction in the human annotator time required to trace the processes of sample neurons (Liu, 2011). Nevertheless, the DIADEM challenge succeeded in focusing computational efforts on automated neuron reconstruction and in producing datasets against which algorithms could be benchmarked.

The complete reconstruction of axonal projections from whole-brain datasets containing multiple labeled neurons is a more demanding problem than that addressed in the DIADEM challenge. Nevertheless, both continued algorithmic development spurred by this effort (Acciai, Soda, & Iannello, 2016; Donohue & Ascoli, 2011; Peng et al., 2015) and improvements in the resolution and clarity of image volumes (Economo et al., 2016; Gong et al., 2013) now enable semiautomated reconstruction. In this paradigm, axonal segments identified algorithmically—even if incomplete—can be utilized as a prior for manual reconstruction, substantially reducing annotation time.

2.4 | Reconstruction validation

Published axonal reconstructions of the same cell types often vary greatly in their extent (e.g., Economo et al., 2018; Gong et al., 2016; Kita & Kita, 2012). This discrepancy is a product of commensurate variability in reconstruction completeness, and likely, accuracy. The problem is exacerbated by the custom of including only skeletonized reconstructions in published studies, which are difficult to assess for completeness and accuracy. The completeness and accuracy of reconstructions within each study can be assessed by comparing reconstructions of the same neuron across multiple annotators (or algorithms) (Winnubst et al., 2019). Across studies, consistency would be enhanced by presentation of representative primary data in publications (Economo et al., 2016) and adopting standards for sharing and visualizing large datasets.

3 | APPLICATIONS

Single neuron axonal reconstructions have been instrumental in determining the precise structure of projection pathways. Here, we highlight two examples in which this information has provided the basis for differentiating cell types and motivating mechanistic hypotheses of circuit function.

3.1 | Striatal pathways

Medium spiny neurons (MSNs) in the striatum were long considered a single cell type (Fox & Rafols, 1975) based on the homogeneity of their somato-dendritic morphology. However, retrograde labeling (Féger & Crossman, 1984; Loopuijt & van der Kooy, 1985; Parent,

Bouchard, & Smith, 1984) and patterned expression of the neuropeptides enkephalin, substance P, and dynorphin (Beckstead & Kersey, 1985; Gerfen & Young, 1988) suggested that MSNs might comprise multiple types. The number of MSN types and their projection targets remained unclear until Kawaguchi and colleagues were able to reconstruct the axons of several cells using classical serial-section histological procedures (Kawaguchi, Wilson, & Emson, 1990). Axonal projection patterns revealed two principal MSN types: direct pathway MSNs target the globus pallidus, entopeduncular nucleus, and substantia nigra while indirect-pathway MSNs connect exclusively with the globus pallidus (Kawaguchi et al., 1990).

The discovery of distinct populations of MSNs, their axonal targets, and their molecular identity directly led to the hypothesis that direct- and indirect-pathway neurons promote and suppress movement initiation respectively (DeLong, 1990; Gerfen et al., 1990). This idea provided a parsimonious explanation for the deficits observed in movement disorders including Huntington's disease and Parkinson's disease and remains the dominant model for the involvement of basal ganglia circuits in motor function. Axonal reconstructions of MSNs were enabled by the relative simplicity of their projection patterns, extending only to targets within the basal ganglia. Complete reconstructions of more complex neurons in other brain areas remained difficult to achieve before whole-brain imaging methods were developed.

3.2 | Pyramidal tract pathways

Cortical pyramidal tract (PT) neurons form the only direct connections between the neocortex and the midbrain, hindbrain, and spinal cord (Lemon, 2008; Shepherd, 2013). PT neurons in the motor cortex communicate cortical motor commands to subcortical motor centers (Dum & Strick, 1991; Evarts, 1966, 1968; Lawrence & Kuypers, 1968; Tower, 1940). Many PT neurons are also activated during the preparation of specific motor actions, well in advance of movement initiation (Tanji & Evarts, 1976) raising the question of why some PT activity patterns drive movement and others do not. The functional heterogeneity of PT neurons is mirrored by their structural diversity. Subsets of PT neurons project to the thalamus, superior colliculus, red nucleus, pons, medulla, and spinal cord (Akintunde & Buxton, 1992; Catsman-Berrevoets & Kuypers, 1981; Hallman, Schofield, & Lin, 1988). Nevertheless, the precise number of PT projection types and their brain-wide connectivity remained unclear.

Brain-wide reconstructions of PT neurons using modern methods (Economo et al., 2016) identified that these neurons could be divided into two groups based on their brain-wide connectivity (Economo et al., 2018). One group of neurons projected to the thalamus—thought to be a critical node for motor planning (Guo et al., 2017)—and avoided the medulla and spinal cord (Figure 4; *green hues*), which contain premotor circuits. The other type displayed the opposite pattern—bypassing the thalamus and branched widely within premotor-nuclei in the medulla (Figure 4; *magenta hues*). Further investigation revealed that thalamus- and medulla-projecting PT neurons are located in distinct cortical laminae and possessed unique gene expression patterns (Economo et al., 2018; Tasic et al., 2018)—establishing that PT neurons consist of two unique cell types. Electrophysiological recordings revealed distinct activity patterns within these two cell types. PT neurons connecting to the thalamus

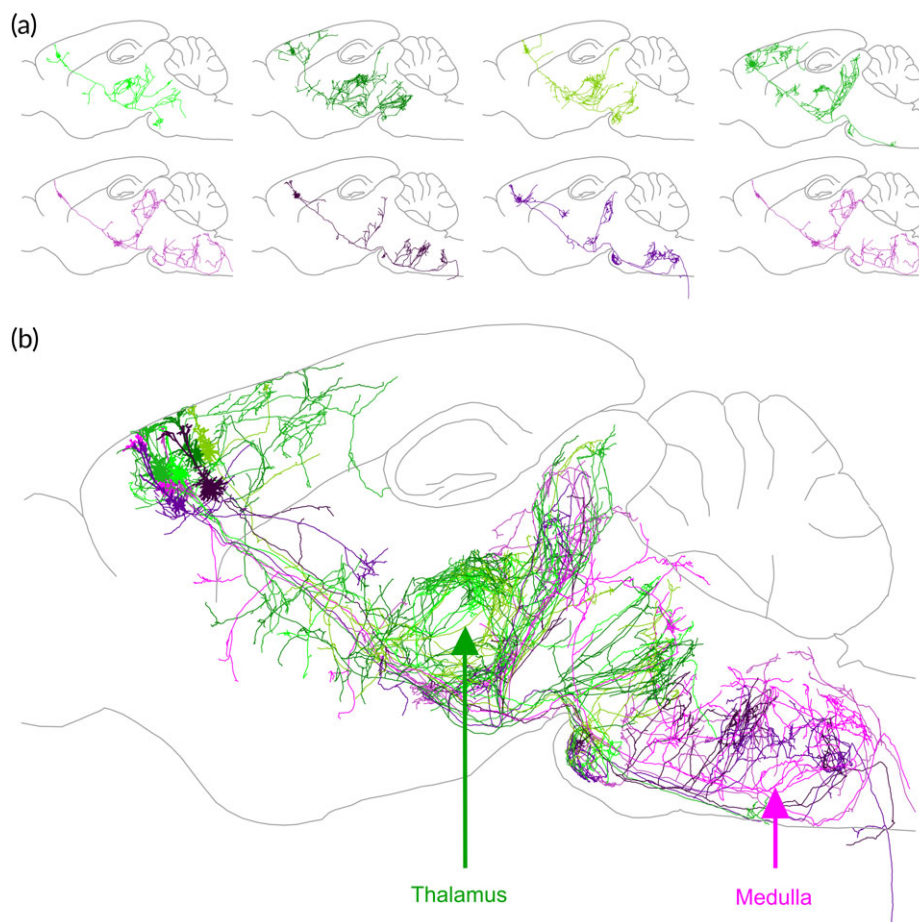


FIGURE 4 Axonal reconstructions of PT neurons reveals their structural diversity. (a) Reconstruction of four thalamus-projecting PT neurons (green hues; top) and four medulla-projecting PT neurons (magenta hues; bottom) collapsed in the sagittal plane. (b) Overlay of the same eight neurons illustrated in (a) reveal that projections to these structures originate from distinct neuronal populations. Adapted from Economo et al. (2018) [Color figure can be viewed at wileyonlinelibrary.com]

stably encode a motor plan for upcoming movements, while PT cells projecting to the medulla communicate motor signals to premotor areas (Economo et al., 2018). These findings delineated novel cortical motor pathways each engaged in distinct phases of movement control.

4 | FUTURE DIRECTIONS

Analyses of single-neuron axonal projections have typically been limited to reconstructions of a few or, at most, a few tens of neurons. Recent technological advances now permit the reconstruction of hundreds or thousands of neurons (Winnubst et al., 2019), an increase of more than a factor of ten. How many neuronal reconstructions will be required to identify all projection neuron types in the brain and to describe their brain-wide connectivity patterns? The mammalian brain contains hundreds of brain areas. In well-studied regions like the mouse neocortex, multiple projection types have been described (Gerfen, Economo, & Chandrashekar, 2018; Shepherd, 2013). To conclude that all projection types have been identified and to characterize the variability within each type, one would like to reconstruct dozens of neurons of each type and hence a hundred or more from each brain area. This implies that a census of tens of thousands of neurons spanning the brain may be required to achieve a description of region-to-region connectivity in the

mammalian brain at a single-neuron level. The eventual attainment of this goal will require an additional increase in axonal reconstruction throughput of at least another order of magnitude. In addition to the current limitations on reconstruction throughput, it remains difficult to evaluate the gene expression and function of neurons whose axons have been reconstructed—other criteria which are critically important for enumerating cell types and understanding the function of neural circuits. These challenges may be addressed by exploiting innovative methodologies.

4.1 | Increasing the throughput of current approaches

One approach for increasing the efficiency of axonal reconstructions is to improve each component of the existing *labeling-imaging-tracing* procedure for axonal reconstruction without altering the overall paradigm.

Improved labeling methods permit more neurons to be labeled and imaged within each brain without increasing the probability of reconstruction errors. Spectral multiplexing greatly reduces the ambiguity introduced by axonal crossovers when axons originating from different cells as each fluoresce with a characteristic color. Although multicolor labeling and imaging has been employed in the past, it has

largely been limited to two distinct fluorophores. Combinatorial labeling with more fluorophores spanning the palette of available colors (Jefferis & Livet, 2012; Lichtman, Livet, & Sanes, 2008), and exhibiting distinct patterns of subcellular localization (Loulrier et al., 2014) could permit many more neurons to be labeled without introducing additional reconstruction ambiguity.

Controlling the spatial distribution of sparsely labeled neurons can further minimize axonal crossovers. The most common approach for sparsely labeling a small cohort of neurons is through viral infection of a subset of neurons within one or a few localized areas (Economo et al., 2016; Kuramoto et al., 2009, 2017; Li et al., 2018; Ohno et al., 2012; Winnubst et al., 2019). Distributing labeled neurons uniformly across the brain minimizes the probability of axonal crossovers, as neurons from different brain regions are less likely to share similar projections than neurons confined to a single region. New viral reagents engineered to efficiently cross the blood brain barrier can be administered systemically and label neurons in this fashion (Bedbrook, Deverman, & Gradinaru, 2018; Chan et al., 2017). Tamoxifen-inducible expression systems and other transgenic approaches provide potential alternatives for sparse, distributed labeling (Lu & Yang, 2017; Wu et al., 2014).

Whole-brain clearing and immunolabeling procedures (Cai et al., 2018; Chung & Deisseroth, 2013; Dodt et al., 2007; Hama et al., 2015; Renier et al., 2014; Richardson & Lichtman, 2015; Susaki et al., 2014; Yang et al., 2014) now enable fast, large volume SPIM imaging. Although the axial resolution of SPIM has lagged that achievable with STPT and KESM/fMOST, this drawback may be addressed by advanced SPIM techniques that overcome limitations on axial resolution (Chhetri et al., 2015; Keller & Dodt, 2012; Keller et al., 2010; Tomer, Khairy, Amat, & Keller, 2012; Verveer et al., 2007). It may be possible to acquire whole mouse brain image volumes with submicron resolution in as little as a few hours using SPIM, an increase of ~50× in acquisition speed compared to STPT and KESM/fMOST.

Together, improved labeling and imaging methods could enable high-resolution whole-brain imaging and reconstruction of hundreds of neurons per day. Exploiting a high-throughput imaging strategy such as SPIM would enable one to image more brains, each containing a lower density of labeled cells. Utilizing a spectrally and spatially distributed labeling strategy would further reduce the effective density of neurons containing the same label. In this regime, ambiguous axonal crossovers could be greatly reduced or eliminated entirely. This strategy, together with continued improvement of automated segmentation and tracing algorithms that fully exploit GPU-accelerated machine learning approaches might allow reconstruction with minimal manual intervention. Analogous approaches for electron microscopy datasets have been successful in reducing reconstruction time, spurred by several public competitions (http://brainiac2.mit.edu/isbi_challenge/; <https://cremi.org/>). Such advances would greatly increase reconstruction throughput and support the determination of the brain-wide connectivity projection neuron types spanning hundreds of brain areas.

4.2 | Sequencing-based analysis of projection patterns

Another class of approaches for revealing long-range connectivity hopes to exploit the low cost and parallelizability of next-generation sequencing

to replace large-scale imaging. In one approach, referred to as MapSeq (Han et al., 2018; Kebschull et al., 2016), viral vectors are synthesized in which each virion expresses a unique sequence ("barcode") together with an axonal targeting sequence. Following an injection of a library of barcoded viral particles, putative target areas are microdissected and sequenced in bulk. The presence or absence of a particular barcode in each target region indicates whether or not that area received a projection from the cell associated with that barcode. The output of a MapSeq experiment is a binary connectivity matrix describing which neurons connect with each brain region. This inexpensive approach makes it possible to evaluate the connectivity of many neurons with many target regions. However, to achieve a high concentration of mRNA barcodes, MapSeq employs viral reagents that are highly toxic to neurons. Additionally, the sensitivity of this method—how much axon must be present in the sequenced sample for the detection of barcode mRNA—remains unclear. While producing some of the same biological information as axonal reconstruction, the spatial resolution of MapSeq is relatively poor and limited to volumes of tissue that can be microdissected. Furthermore, this approach is largely unable to assess the spatial distribution of axonal projections within a target area and provides only coarse information about the extent of innervation. Nevertheless, sequencing based methods such as MapSeq offer an exciting, complementary approaches to the *labeling-imaging-tracing* paradigm for projection mapping.

4.3 | Physiological and transcriptomic analysis of reconstructed neurons

A consensus set of cell types in the brain will ultimately be synthesized from a combination of morphological, transcriptomic, and physiological descriptors. Large-scale efforts are rapidly identifying and cataloguing transcriptomic cell types—groups of neurons exhibiting similar gene expression patterns—across the brain (Saunders et al., 2018; Tasic et al., 2018; Zeisel et al., 2018). Integrating information about a neuron's gene expression and physiology with axonal reconstructions remains a major outstanding challenge.

Gene expression patterns of reconstructed neurons may be determined through a number of approaches. Projection patterns may be characterized within genetically specified populations by taking advantage of transgenic driver lines (Gong et al., 2007; Madisen et al., 2010). A more complete representation of gene expression within each neuron can be provided by combining axonal reconstruction with *in situ* hybridization (ISH) of multiple transcripts. These efforts are hindered by the difficulty of performing ISH in whole-brain tissue volumes, although progress has been made toward this goal (Chen et al., 2016; Lein, Borm, & Linnarsson, 2017; Shah et al., 2016). Alternately, tissue sections removed during whole-brain STPT may be collected following imaging (Jiang et al., 2017) and processed for ISH to reveal the molecular identity of imaged neurons. This approach can leverage existing gene expression datasets produced using single-cell RNA sequencing methods. In-depth surveys of the expression patterns of all transcriptomic types in a brain region can be mined for a small set of genes whose expression effectively discriminates between types. ISH may then be used to determine the expression of the reduced set to map each cell onto a particular transcriptomic type.

Neurons may be characterized physiologically before axonal reconstruction using electrophysiological or optical recording techniques. Similar to classical methods for staining neurons during patch clamp recordings, a glass pipette can be used to both record neuronal activity and deliver plasmid DNA encoding a fluorescent protein (Cohen et al., 2013; Han et al., 2018; Kitamura, Judkewitz, Kano, Denk, & Häusser, 2008; Rancz et al., 2011) that can be used for post hoc axonal reconstruction. Due to experimental challenges, this process is typically limited to small numbers of neurons near the dorsal surface of the brain.

Optical recording methods in which activity is reported by genetically encoded calcium or voltage indicators (GECIs/GEVIs) (Chen et al., 2013; Hochbaum et al., 2014; Lin & Schnitzer, 2016; Sepelri Rad et al., 2017) can also be used to characterize neurons physiologically prior to axonal reconstruction. In this paradigm, GECIs/GEVIs may be expressed densely within a given brain region so that a large population of cells can be functionally characterized. A second, spectrally distinct fluorophore may then be expressed sparsely in a subset of cells and used for post hoc axonal reconstruction.

5 | CONCLUSIONS

Understanding region-to-region connectivity in the mammalian brain is the underlying motivation for a number of large-scale efforts in mice (Bohland et al., 2009; Oh et al., 2014), and humans (Glasser et al., 2016; Van Essen et al., 2013). Nevertheless, little is known about the fine structure of brain-wide connectivity at the single neuron level—the structural substrate controlling how information flows between brain areas. Application of innovative methodology to improve the speed, accuracy, and completeness of axonal reconstruction is addressing this knowledge gap and illuminating the pathways through which information is broadcasted from the hippocampus (Cembrowski et al., 2018), motor cortex (Economo et al., 2018; Hooks et al., 2018), and thalamus (Phillips et al., 2018) to the rest of the brain. A systematic brain wide analysis of projection pathways may soon be possible through the continued exploitation of advances in computational, optical, and genetic tools.

ACKNOWLEDGMENTS

We would like to thank Karel Svoboda and Nelson Spruston for helpful discussions and Tim Wang, Nathan Clack, and Daniel Turner-Evans for critical comments on the manuscript. The authors were supported by the Howard Hughes Medical Institute.

ORCID

Michael N. Economo  <https://orcid.org/0000-0001-9893-1505>

Tiago A. Ferreira  <https://orcid.org/0000-0001-6866-1540>

REFERENCES

Acciai, L., Soda, P., & Iannello, G. (2016). Automated neuron tracing methods: An updated account. *Neuroinformatics*, 14(4), 353–367. <https://doi.org/10.1007/s12021-016-9310-0>

Akintunde, A., & Buxton, D. F. (1992). Origins and collateralization of corticospinal, corticopontine, corticorubral and corticostriatal tracts: A multiple retrograde fluorescent tracing study. *Brain Research*, 586(2), 208–218.

Ascoli, G. A. (2008). Neuroinformatics grand challenges. *Neuroinformatics*, 6(1), 1–3. <https://doi.org/10.1007/s12021-008-9010-5>

Beckstead, R. M., & Kersey, K. S. (1985). Immunohistochemical demonstration of differential substance P-, met-enkephalin-, and glutamic-acid-decarboxylase-containing cell body and axon distributions in the corpus striatum of the cat. *The Journal of Comparative Neurology*, 232(4), 481–498. <https://doi.org/10.1002/cne.902320406>

Bedbrook, C. N., Deverman, B. E., & Gradinaru, V. (2018). Viral strategies for targeting the central and peripheral nervous systems. *Annual Review of Neuroscience*, 41, 323–348. <https://doi.org/10.1146/annurev-neuro-080317-062048>

Bock, D. D., Lee, W.-C. A., Kerlin, A. M., Andermann, M. L., Hood, G., Wetzel, A. W., ... Reid, R. C. (2011). Network anatomy and in vivo physiology of visual cortical neurons. *Nature*, 471(7337), 177–182. <https://doi.org/10.1038/nature09802>

Bohland, J. W., Wu, C., Barbas, H., Bokil, H., Bota, M., Breiter, H. C., ... Mitra, P. P. (2009). A proposal for a coordinated effort for the determination of brainwide neuroanatomical connectivity in model organisms at a mesoscopic scale. *PLoS Computational Biology*, 5(3), e1000334. <https://doi.org/10.1371/journal.pcbi.1000334>

Cai, R., Pan, C., Ghasemigharagoz, A., Todorov, M. I., Foerster, B., Zhao, S., & Erturk, A. (2018). Panoptic vDISCO imaging reveals neuronal connectivity, remote trauma effects and meningeal vessels in intact transparent mice. *BioRxiv*, 374785. doi:<https://doi.org/10.1101/374785>.

Catsman-Berrevoets, C. E., & Kuypers, H. G. (1981). A search for corticospinal collaterals to thalamus and mesencephalon by means of multiple retrograde fluorescent tracers in cat and rat. *Brain Research*, 218(1–2), 15–33.

Cembrowski, M. S., Phillips, M. G., DiLisio, S. F., Shields, B. C., Winnubst, J., Chandrashekar, J., ... Spruston, N. (2018). Dissociable structural and functional hippocampal outputs via distinct subiculum cell classes. *Cell*, 173(5), 1280–1292.e18. <https://doi.org/10.1016/j.cell.2018.03.031>

Chan, K. Y., Jang, M. J., Yoo, B. B., Greenbaum, A., Ravi, N., Wu, W.-L., ... Gradinaru, V. (2017). Engineered AAVs for efficient noninvasive gene delivery to the central and peripheral nervous systems. *Nature Neuroscience*, 20(8), 1172–1179. <https://doi.org/10.1038/nn.4593>

Chen, F., Wassie, A. T., Cote, A. J., Sinha, A., Alon, S., Asano, S., ... Boyden, E. S. (2016). Nanoscale imaging of RNA with expansion microscopy. *Nature Methods*, 13(8), 679–684. <https://doi.org/10.1038/nmeth.3899>

Chen, T.-W., Wardill, T. J., Sun, Y., Pulver, S. R., Renninger, S. L., Baohuan, A., ... Kim, D. S. (2013). Ultrasensitive fluorescent proteins for imaging neuronal activity. *Nature*, 499(7458), 295–300. <https://doi.org/10.1038/nature12354>

Chhetri, R. K., Amat, F., Wan, Y., Höckendorf, B., Lemon, W. C., & Keller, P. J. (2015). Whole-animal functional and developmental imaging with isotropic spatial resolution. *Nature Methods*, 12(12), 1171–1178. <https://doi.org/10.1038/nmeth.3632>

Chothani, P., Mehta, V., & Stepanyants, A. (2011). Automated tracing of neurites from light microscopy stacks of images. *Neuroinformatics*, 9(2–3), 263–278. <https://doi.org/10.1007/s12021-011-9121-2>

Chung, K., & Deisseroth, K. (2013). CLARITY for mapping the nervous system. *Nature Methods*, 10(6), 508–513. <https://doi.org/10.1038/nmeth.2481>

Cohen, L., Koffman, N., Meiri, H., Yarom, Y., Lampl, I., & Mizrahi, A. (2013). Time-lapse electrical recordings of single neurons from the mouse neocortex. *Proceedings of the National Academy of Sciences*, 110(14), 5665–5670. <https://doi.org/10.1073/pnas.1214434110>

Cullheim, S., & Kellerth, J.-O. (1976). Combined light and electron microscopic tracing of neurons, including axons and synaptic terminals, after intracellular injection of horseradish peroxidase. *Neuroscience Letters*, 2(6), 307–313. [https://doi.org/10.1016/0304-3940\(76\)90165-8](https://doi.org/10.1016/0304-3940(76)90165-8)

DeLong, M. R. (1990). Primate models of movement disorders of basal ganglia origin. *Trends in Neurosciences*, 13(7), 281–285. [https://doi.org/10.1016/0166-2236\(90\)90110-V](https://doi.org/10.1016/0166-2236(90)90110-V)

Dodt, H.-U., Leischner, U., Schierloh, A., Jährling, N., Mauch, C. P., Deininger, K., ... Becker, K. (2007). Ultramicroscopy: Three-dimensional

- visualization of neuronal networks in the whole mouse brain. *Nature Methods*, 4(4), 331–336. <https://doi.org/10.1038/nmeth1036>
- Donohue, D. E., & Ascoli, G. A. (2011). Automated reconstruction of neuronal morphology: An overview. *Brain Research Reviews*, 67(1–2), 94–102. <https://doi.org/10.1016/j.brainresrev.2010.11.003>
- Dum, R. P., & Strick, P. L. (1991). The origin of corticospinal projections from the premotor areas in the frontal lobe. *Journal of Neuroscience*, 11(3), 667–689. <https://doi.org/10.1523/JNEUROSCI.11-03-00667.1991>
- Economo, M. N., Clack, N. G., Arthur, B. J., Bruns, C., Bas, E., & Chandrashekar, J. (2015). Registration and resampling of large-scale 3D mosaic images. *Proceedings of BioImage Informatics Conference*, 3.
- Economo, M. N., Clack, N. G., Lavis, L. D., Gerfen, C. R., Svoboda, K., Myers, E. W., & Chandrashekar, J. (2016). A platform for brain-wide imaging and reconstruction of individual neurons. *eLife*, 5, e10566. <https://doi.org/10.7554/eLife.10566>
- Economo, M. N., Viswanathan, S., Tasic, B., Bas, E., Winnubst, J., Menon, V., ... Svoboda, K. (2018). Distinct descending motor cortex pathways and their roles in movement. *Nature*, 563, 79–84.
- Evarts, E. V. (1966). Pyramidal tract activity associated with a conditioned hand movement in the monkey. *Journal of Neurophysiology*, 29(6), 1011–1027.
- Evarts, E. V. (1968). Relation of pyramidal tract activity to force exerted during voluntary movement. *Journal of Neurophysiology*, 31(1), 14–27.
- Féger, J., & Crossman, A. R. (1984). Identification of different subpopulations of neostriatal neurones projecting to globus pallidus or substantia nigra in the monkey: A retrograde fluorescence double-labelling study. *Neuroscience Letters*, 49(1–2), 7–12.
- Fox, C. A., & Rafols, J. A. (1975). The radial fibers in the globus pallidus. *The Journal of Comparative Neurology*, 159(2), 177–199. <https://doi.org/10.1002/cne.901590203>
- Gerfen, C. R., Economo, M. N., & Chandrashekar, J. (2018). Long distance projections of cortical pyramidal neurons. *Journal of Neuroscience Research*, 96(9), 1467–1475. <https://doi.org/10.1002/jnr.23978>
- Gerfen, C. R., Engber, T. M., Mahan, L. C., Susel, Z., Chase, T. N., Monsma, F. J., & Sibley, D. R. (1990). D1 and D2 dopamine receptor-regulated gene expression of striatonigral and striatopallidal neurons. *Science (New York, N.Y.)*, 250(4986), 1429–1432.
- Gerfen, C. R., & Young, S. W. (1988). Distribution of striatonigral and striatopallidal peptidergic neurons in both patch and matrix compartments: An in situ hybridization histochemistry and fluorescent retrograde tracing study. *Brain Research*, 460(1), 161–167. [https://doi.org/10.1016/0006-8993\(88\)91217-6](https://doi.org/10.1016/0006-8993(88)91217-6)
- Glaser, E. M., & Loos, H. V. D. (1965). A semi-automatic computer-microscope for the analysis of neuronal morphology. *IEEE Transactions on Biomedical Engineering*, 12(1), 22–31. <https://doi.org/10.1109/TBME.1965.4502337>
- Glasser, M. F., Smith, S. M., Marcus, D. S., Andersson, J. L. R., Auerbach, E. J., Behrens, T. E. J., ... Essen, D. C. V. (2016). The human connectome project's neuroimaging approach. *Nature Neuroscience*, 19(9), 1175–1187. <https://doi.org/10.1038/nn.4361>
- Golgi, C. (1873). Sulla sostanza grigia del cervello. *Gazzetta Medica Italiana*, 33, 244–246.
- Gong, H., Xu, D., Yuan, J., Li, X., Guo, C., Peng, J., & Luo, Q. (2016). High-throughput dual-colour precision imaging for brain-wide connectome with cytoarchitectonic landmarks at the cellular level. *Nature Communications*, 7, 12142. <https://doi.org/10.1038/ncomms12142>
- Gong, H., Zeng, S., Yan, C., Lv, X., Yang, Z., Xu, T., ... Luo, Q. (2013). Continuously tracing brain-wide long-distance axonal projections in mice at a one-micron voxel resolution. *NeuroImage*, 74, 87–98. <https://doi.org/10.1016/j.neuroimage.2013.02.005>
- Gong, S., Doughty, M., Harbaugh, C. R., Cummins, A., Hatten, M. E., Heintz, N., & Gerfen, C. R. (2007). Targeting Cre recombinase to specific neuron populations with bacterial artificial chromosome constructs. *The Journal of Neuroscience: The Official Journal of the Society for Neuroscience*, 27(37), 9817–9823. <https://doi.org/10.1523/JNEUROSCI.2707-07.2007>
- Guo, Z. V., Inagaki, H. K., Daie, K., Druckmann, S., Gerfen, C. R., & Svoboda, K. (2017). Maintenance of persistent activity in a frontal thalamocortical loop. *Nature*, 545(7653), 181–186. <https://doi.org/10.1038/nature22324>
- Hallman, L. E., Schofield, B. R., & Lin, C.-S. (1988). Dendritic morphology and axon collaterals of corticotectal, corticopontine, and callosal neurons in layer V of primary visual cortex of the hooded rat. *Journal of Comparative Neurology*, 272(1), 149–160. <https://doi.org/10.1002/cne.902720111>
- Hama, H., Hioki, H., Namiki, K., Hoshida, T., Kurokawa, H., Ishidate, F., ... Miyawaki, A. (2015). ScaleS: An optical clearing palette for biological imaging. *Nature Neuroscience*, 18(10), 1518–1529. <https://doi.org/10.1038/nn.4107>
- Han, Y., Kebschull, J. M., Campbell, R. A. A., Cowan, D., Imhof, F., Zador, A. M., & Mrsic-Flogel, T. D. (2018). The logic of single-cell projections from visual cortex. *Nature*, 556(7699), 51–56. <https://doi.org/10.1038/nature26159>
- Helmstaedter, M., Briggman, K. L., Turaga, S. C., Jain, V., Seung, H. S., & Denk, W. (2013). Connectomic reconstruction of the inner plexiform layer in the mouse retina. *Nature*, 500(7461), 168–174. <https://doi.org/10.1038/nature12346>
- Hochbaum, D. R., Zhao, Y., Farhi, S. L., Klapoetke, N., Werley, C. A., Kapoor, V., ... Cohen, A. E. (2014). All-optical electrophysiology in mammalian neurons using engineered microbial rhodopsins. *Nature Methods*, 11(8), 825–833. <https://doi.org/10.1038/nmeth.3000>
- Hooks, B. M., Papale, A. E., Paletzki, R. F., Feroze, M. W., Eastwood, B. S., Couey, J. J., & Gerfen, C. R. (2018). Topographic precision in sensory and motor corticostriatal projections varies across cell type and cortical area. *Nature Communications*, 9(1), 3549. <https://doi.org/10.1038/s41467-018-05780-7>
- Horikawa, K., & Armstrong, W. E. (1988). A versatile means of intracellular labeling: Injection of biocytin and its detection with avidin conjugates. *Journal of Neuroscience Methods*, 25(1), 1–11.
- Jefferis, G. S., & Livet, J. (2012). Sparse and combinatorial neuron labelling. *Current Opinion in Neurobiology*, 22(1), 101–110. <https://doi.org/10.1016/j.conb.2011.09.010>
- Jiang, T., Long, B., Gong, H., Xu, T., Li, X., Duan, Z., & Yuan, J. (2017). A platform for efficient identification of molecular phenotypes of brain-wide neural circuits. *Scientific Reports*, 7(1), 13891. <https://doi.org/10.1038/s41598-017-14360-6>
- Kasthuri, N., Hayworth, K. J., Berger, D. R., Schalek, R., Conchello, J. A., Knowles-Barley, S., ... Lichtman, J. W. (2015). Saturated reconstruction of a volume of neocortex. *Cell*, 162, 648–661. <https://doi.org/10.1016/j.cell.2015.06.054>
- Kawaguchi, Y., Wilson, C. J., & Emson, P. C. (1990). Projection subtypes of rat neostriatal matrix cells revealed by intracellular injection of biocytin. *The Journal of Neuroscience: The Official Journal of the Society for Neuroscience*, 10(10), 3421–3438.
- Kebschull, J. M., Garcia da Silva, P., Reid, A. P., Peikon, I. D., Albeanu, D. F., & Zador, A. M. (2016). High-throughput mapping of single-neuron projections by sequencing of barcoded RNA. *Neuron*, 91(5), 975–987. <https://doi.org/10.1016/j.neuron.2016.07.036>
- Keller, P. J., & Dodt, H.-U. (2012). Light sheet microscopy of living or cleared specimens. *Current Opinion in Neurobiology*, 22(1), 138–143. <https://doi.org/10.1016/j.conb.2011.08.003>
- Keller, P. J., Schmidt, A. D., Santella, A., Khairy, K., Bao, Z., Wittbrodt, J., & Stelzer, E. H. K. (2010). Fast, high-contrast imaging of animal development with scanned light sheet-based structured-illumination microscopy. *Nature Methods*, 7(8), 637–642. <https://doi.org/10.1038/nmeth.1476>
- Kita, T., & Kita, H. (2012). The subthalamic nucleus is one of multiple innervation sites for long-range corticofugal axons: A single-axon tracing study in the rat. *The Journal of Neuroscience: The Official Journal of the Society for Neuroscience*, 32(17), 5990–5999. <https://doi.org/10.1523/JNEUROSCI.5717-11.2012>
- Kitai, S. T., Kocsis, J. D., Preston, R. J., & Sugimori, M. (1976). Monosynaptic inputs to caudate neurons identified by intracellular injection of horseradish peroxidase. *Brain Research*, 109(3), 601–606. [https://doi.org/10.1016/0006-8993\(76\)90039-1](https://doi.org/10.1016/0006-8993(76)90039-1)
- Kitamura, K., Judkewitz, B., Kano, M., Denk, W., & Häusser, M. (2008). Targeted patch-clamp recordings and single-cell electroporation of unlabeled neurons in vivo. *Nature Methods*, 5(1), 61–67. <https://doi.org/10.1038/nmeth1150>
- Kovačević, N., Henderson, J. T., Chan, E., Lifshitz, N., Bishop, J., Evans, A. C., ... Chen, X. J. (2005). A three-dimensional MRI atlas of the mouse brain with estimates of the average and variability. *Cerebral Cortex*, 15(5), 639–645. <https://doi.org/10.1093/cercor/bhh165>

- Kuramoto, E., Furuta, T., Nakamura, K. C., Unzai, T., Hioki, H., & Kaneko, T. (2009). Two types of thalamocortical projections from the motor thalamic nuclei of the rat: A single neuron-tracing study using viral vectors. *Cerebral Cortex* (New York, N.Y.: 1991), 19(9), 2065–2077. <https://doi.org/10.1093/cercor/bhn231>
- Kuramoto, E., Pan, S., Furuta, T., Tanaka, Y. R., Iwai, H., Yamanaka, A., & Hioki, H. (2017). Individual mediodorsal thalamic neurons project to multiple areas of the rat prefrontal cortex: A single neuron-tracing study using virus vectors. *The Journal of Comparative Neurology*, 525(1), 166–185. <https://doi.org/10.1002/cne.24054>
- Lawrence, D. G., & Kuypers, H. G. (1968). The functional organization of the motor system in the monkey. I. The effects of bilateral pyramidal lesions. *Brain: A Journal of Neurology*, 91(1), 1–14.
- Lein, E., Borm, L. E., & Linnarsson, S. (2017). The promise of spatial transcriptomics for neuroscience in the era of molecular cell typing. *Science*, 358(6359), 64–69. <https://doi.org/10.1126/science.aan6827>
- Lemon, R. N. (2008). Descending pathways in motor control. *Annual Review of Neuroscience*, 31, 195–218. <https://doi.org/10.1146/annurev.neuro.31.060407.125547>
- Li, A., Gong, H., Zhang, B., Wang, Q., Yan, C., Wu, J., ... Luo, Q. (2010). Micro-optical sectioning tomography to obtain a high-resolution atlas of the mouse brain. *Science* (New York, N.Y.), 330(6009), 1404–1408. <https://doi.org/10.1126/science.1191776>
- Li, X., Yu, B., Sun, Q., Zhang, Y., Ren, M., Zhang, X., ... Qiu, Z. (2018). Generation of a whole-brain atlas for the cholinergic system and mesoscopic projectome analysis of basal forebrain cholinergic neurons. *Proceedings of the National Academy of Sciences of the United States of America*, 115(2), 415–420. <https://doi.org/10.1073/pnas.1703601115>
- Lichtman, J. W., Livet, J., & Sanes, J. R. (2008). A technicolour approach to the connectome. *Nature Reviews. Neuroscience*, 9(6), 417–422. <https://doi.org/10.1038/nrn2391>
- Lin, M. Z., & Schnitzer, M. J. (2016). Genetically encoded indicators of neuronal activity. *Nature Neuroscience*, 19(9), 1142–1153. <https://doi.org/10.1038/nn.4359>
- Liu, Y. (2011). The DIADEM and beyond. *Neuroinformatics*, 9(2), 99–102. <https://doi.org/10.1007/s12021-011-9102-5>
- Loopuijt, L. D., & van der Kooy, D. (1985). Organization of the striatum: Collateralization of its efferent axons. *Brain Research*, 348(1), 86–99.
- Loulier, K., Barry, R., Mahou, P., Le Franc, Y., Supatto, W., Matho, K. S., ... Livet, J. (2014). Multiplex cell and lineage tracking with combinatorial labels. *Neuron*, 81(3), 505–520. <https://doi.org/10.1016/j.neuron.2013.12.016>
- Lu, X.-H., & Yang, X. W. (2017). Genetically-directed sparse neuronal labeling in BAC transgenic mice through mononucleotide repeat frameshift. *Scientific Reports*, 7, 43915. <https://doi.org/10.1038/srep43915>
- Luo, L., Callaway, E. M., & Svoboda, K. (2008). Genetic dissection of neural circuits. *Neuron*, 57(5), 634–660. <https://doi.org/10.1016/j.neuron.2008.01.002>
- Luo, L., Callaway, E. M., & Svoboda, K. (2018). Genetic dissection of neural circuits: A decade of progress. *Neuron*, 98(2), 256–281. <https://doi.org/10.1016/j.neuron.2018.03.040>
- Madisen, L., Zwingman, T. A., Sunken, S. M., Oh, S. W., Zariwala, H. A., Gu, H., ... Zeng, H. (2010). A robust and high-throughput Cre reporting and characterization system for the whole mouse brain. *Nature Neuroscience*, 13(1), 133–140. <https://doi.org/10.1038/nn.2467>
- Mayerich, D., Abbott, L., & McCormick, B. (2008). Knife-edge scanning microscopy for imaging and reconstruction of three-dimensional anatomical structures of the mouse brain. *Journal of Microscopy*, 231(Pt 1), 134–143. <https://doi.org/10.1111/j.1365-2818.2008.02024.x>
- Meijering, E. (2010). Neuron tracing in perspective. *Cytometry Part A*, 77A(7), 693–704. <https://doi.org/10.1002/cyto.a.20895>
- Mertz, J. (2011). Optical sectioning microscopy with planar or structured illumination. *Nature Methods*, 8(10), 811–819. <https://doi.org/10.1038/nmeth.1709>
- Oh, S. W., Harris, J. A., Ng, L., Winslow, B., Cain, N., Mihalas, S., ... Zeng, H. (2014). A mesoscale connectome of the mouse brain. *Nature*, 508(7495), 207–214. <https://doi.org/10.1038/nature13186>
- Ohno, S., Kuramoto, E., Furuta, T., Hioki, H., Tanaka, Y. R., Fujiyama, F., & Kaneko, T. (2012). A morphological analysis of thalamocortical axon fibers of rat posterior thalamic nuclei: A single neuron tracing study with viral vectors. *Cerebral Cortex* (New York, N.Y.: 1991), 22(12), 2840–2857. <https://doi.org/10.1093/cercor/bhr356>
- Parent, A., Bouchard, C., & Smith, Y. (1984). The striatopallidal and striatonigral projections: Two distinct fiber systems in primate. *Brain Research*, 303(2), 385–390. [https://doi.org/10.1016/0006-8993\(84\)91224-1](https://doi.org/10.1016/0006-8993(84)91224-1)
- Peng, H., Hawrylycz, M., Roskams, J., Hill, S., Spruston, N., Meijering, E., & Ascoli, G. A. (2015). BigNeuron: Large-scale 3D neuron reconstruction from optical microscopy images. *Neuron*, 87(2), 252–256. <https://doi.org/10.1016/j.neuron.2015.06.036>
- Phillips, J. W., Schulmann, A., Hara, E., Liu, C., Wang, L., Shields, B., ... Hantman, A. (2018). A single spectrum of neuronal identities across thalamus. *BioRxiv*, 241315. <https://doi.org/10.1101/241315>
- Quan, T., Zhou, H., Li, J., Li, S., Li, A., Li, Y., ... Zeng, S. (2016). NeuroGPS-tree: Automatic reconstruction of large-scale neuronal populations with dense neurites. *Nature Methods*, 13(1), 51–54. <https://doi.org/10.1038/nmeth.3662>
- Ragan, T., Kadiri, L. R., Venkataraju, K. U., Bahlmann, K., Sutin, J., Taranda, J., ... Osten, P. (2012). Serial two-photon tomography for automated ex vivo mouse brain imaging. *Nature Methods*, 9(3), 255–258. <https://doi.org/10.1038/nmeth.1854>
- Ramón y Cajal, S. (1888). Estructura de los centros nerviosos de las aves.
- Ramón y Cajal, S. (1891). *Sur la structure de l'écorce cérébrale de quelques mammifères*. Typ. de Joseph van In & Cie.; Aug. Peeters, lib.
- Rancz, E. A., Franks, K. M., Schwarz, M. K., Pichler, B., Schaefer, A. T., & Margrie, T. W. (2011). Transfection via whole-cell recording in vivo: Bridging single-cell physiology, genetics and connectomics. *Nature Neuroscience*, 14(4), 527–532. <https://doi.org/10.1038/nn.2765>
- Renier, N., Wu, Z., Simon, D. J., Yang, J., Ariel, P., & Tessier-Lavigne, M. (2014). iDISCO: A simple, rapid method to immunolabel large tissue samples for volume imaging. *Cell*, 159(4), 896–910. <https://doi.org/10.1016/j.cell.2014.10.010>
- Richardson, D. S., & Lichtman, J. W. (2015). Clarifying tissue clearing. *Cell*, 162(2), 246–257. <https://doi.org/10.1016/j.cell.2015.06.067>
- Ropiredy, D., Scorcioni, R., Lasher, B., Buzsáki, G., & Ascoli, G. A. (2011). Axonal morphometry of hippocampal pyramidal neurons semi-automatically reconstructed after in vivo labeling in different CA3 locations. *Brain Structure & Function*, 216(1), 1–15. <https://doi.org/10.1007/s00429-010-0291-8>
- Saunders, A., Macosko, E. Z., Wysoker, A., Goldman, M., Krienen, F. M., de Rivera, H., ... McCarroll, S. A. (2018). Molecular diversity and specializations among the cells of the adult mouse brain. *Cell*, 174(4), 1015–1030.e16. <https://doi.org/10.1016/j.cell.2018.07.028>
- Scorcioni, R., & Ascoli, G. A. (2005). Algorithmic reconstruction of complete axonal arborizations in rat hippocampal neurons. *Neurocomputing*, 65–66, 15–22. <https://doi.org/10.1016/j.neucom.2004.10.105>
- Sepehri Rad, M., Choi, Y., Cohen, L. B., Baker, B. J., Zhong, S., Storace, D. A., & Braubach, O. R. (2017). Voltage and calcium imaging of brain activity. *Biophysical Journal*, 113(10), 2160–2167. <https://doi.org/10.1016/j.bpj.2017.09.040>
- Shah, S., Lubbeck, E., Schwarzkopf, M., He, T.-F., Greenbaum, A., Sohn, C. H., ... Cai, L. (2016). Single-molecule RNA detection at depth by hybridization chain reaction and tissue hydrogel embedding and clearing. *Development* (Cambridge, England), 143(15), 2862–2867. <https://doi.org/10.1242/dev.138560>
- Shepherd, G. M., & Harris, K. M. (1998). Three-dimensional structure and composition of CA3→CA1 axons in rat hippocampal slices: Implications for presynaptic connectivity and compartmentalization. *The Journal of Neuroscience: The Official Journal of the Society for Neuroscience*, 18(20), 8300–8310.
- Shepherd, G. M. G. (2013). Corticostriatal connectivity and its role in disease. *Nature Reviews. Neuroscience*, 14(4), 278–291. <https://doi.org/10.1038/nrn3469>
- Snow, P. J., Rose, P. K., & Brown, A. G. (1976). Tracing axons and axon collaterals of spinal neurons using intracellular injection of horseradish peroxidase. *Science*, 191(4224), 312–313. <https://doi.org/10.1126/science.54936>
- Stewart, W. W. (1978). Functional connections between cells as revealed by dye-coupling with a highly fluorescent naphthalimide tracer. *Cell*, 14(3), 741–759.
- Stuart, G. J., Dodt, H. U., & Sakmann, B. (1993). Patch-clamp recordings from the soma and dendrites of neurons in brain slices using infrared

- video microscopy. *Pflügers Archiv: European Journal of Physiology*, 423 (5–6), 511–518.
- Susaki, E. A., Tainaka, K., Perrin, D., Kishino, F., Tawara, T., Watanabe, T. M., ... Ueda, H. R. (2014). Whole-brain imaging with single-cell resolution using chemical cocktails and computational analysis. *Cell*, 157(3), 726–739. <https://doi.org/10.1016/j.cell.2014.03.042>
- Tanji, J., & Evarts, E. V. (1976). Anticipatory activity of motor cortex neurons in relation to direction of an intended movement. *Journal of Neurophysiology*, 39(5), 1062–1068.
- Tasic, B., Yao, Z., Smith, K., Graybiel, L., Nguyen, T., Bertagnolli, D., ... Koch, C. (2018). Shared and distinct transcriptomic cell types across neocortical areas. *Nature*, 563(7729), 72–78. <https://doi.org/10.1038/s41586-018-0654-5>
- Tomer, R., Khairy, K., Amat, F., & Keller, P. J. (2012). Quantitative high-speed imaging of entire developing embryos with simultaneous multi-view light-sheet microscopy. *Nature Methods*, 9(7), 755–763. <https://doi.org/10.1038/nmeth.2062>
- Tower, S. S. (1940). Pyramidal lesion in the monkey. *Brain*, 63(1), 36–90. <https://doi.org/10.1093/brain/63.1.36>
- Van Essen, D. C., Smith, S. M., Barch, D. M., Behrens, T. E. J., Yacoub, E., & Ugurbil, K. (2013). The WU-Minn human connectome project: An overview. *NeuroImage*, 80, 62–79. <https://doi.org/10.1016/j.neuroimage.2013.05.041>
- Verveer, P. J., Swoger, J., Pampaloni, F., Greger, K., Marcello, M., & Stelzer, E. H. K. (2007). High-resolution three-dimensional imaging of large specimens with light sheet-based microscopy. *Nature Methods*, 4 (4), 311–313. <https://doi.org/10.1038/nmeth1017>
- Voie, A. H., Burns, D. H., & Spelman, F. A. (1993). Orthogonal-plane fluorescence optical sectioning: Three-dimensional imaging of macroscopic biological specimens. *Journal of Microscopy*, 170Pt 3, 229–236.
- Winnubst, J., Bas, E., Ferreira, T. A., Wu, Z., Economo, M. N., Edson, P., & Chandrashekar, J. (2019). Reconstruction of 1,000 projection neurons reveals new cell types and organization of long-range connectivity in the mouse brain. *BioRxiv*, 537233. <https://doi.org/10.1101/537233>
- Wittner, L., Henze, D. A., Záborszky, L., & Buzsáki, G. (2007). Three-dimensional reconstruction of the axon arbor of a CA3 pyramidal cell recorded and filled in vivo. *Brain Structure & Function*, 212(1), 75–83. <https://doi.org/10.1007/s00429-007-0148-y>
- Wu, H., Williams, J., & Nathans, J. (2014). Complete morphologies of basal forebrain cholinergic neurons in the mouse. *eLife*, 3, e02444.
- Xiong, H., Zhou, Z., Zhu, M., Lv, X., Li, A., Li, S., ... Zeng, S. (2014). Chemical reactivation of quenched fluorescent protein molecules enables resin-embedded fluorescence microimaging. *Nature Communications*, 5, 3992. <https://doi.org/10.1038/ncomms4992>
- Yang, B., Treweek, J. B., Kulkarni, R. P., Deverman, B. E., Chen, C.-K., Lubeck, E., ... Gradinaru, V. (2014). Single-cell phenotyping within transparent intact tissue through whole-body clearing. *Cell*, 158(4), 945–958. <https://doi.org/10.1016/j.cell.2014.07.017>
- Zeisel, A., Hochgerner, H., Lönnerberg, P., Johnsson, A., Memic, F., van der Zwan, J., ... Linnarsson, S. (2018). Molecular architecture of the mouse nervous system. *Cell*, 174(4), 999–1014.e22. <https://doi.org/10.1016/j.cell.2018.06.021>

How to cite this article: Economo MN, Winnubst J, Bas E, Ferreira TA, Chandrashekar J. Single-neuron axonal reconstruction: The search for a wiring diagram of the brain. *J Comp Neurol*. 2019;1–10. <https://doi.org/10.1002/cne.24674>